The Cryosphere Discuss., 4, 1877–1908, 2010
www.the-cryosphere-discuss.net/4/1877/2010/
doi:10.5194/tcd-4-1877-2010

The Cryosphere Discussions

Modelling past and future permafrost conditions in Svalbard

B. Etzelmüller[1], T. V. Schuler[1], K. Isaksen[2], H. H. Christiansen[3,1], H. Farbrot[1], and R. Benestad[2]

[1]Department of Geosciences, University of Oslo, Norway, P.O. Box 1047, Blindern, 0316 Oslo, Norway
[2]Norwegian Meteorological Institute, P.O. Box 43, Blindern, 0313 Oslo, Norway
[3]The University Centre in Svalbard (UNIS), P.O. Box 156, 9171 Longyearbyen, Norway

Received: 24 August 2010 – Accepted: 3 September 2010 – Published: 4 October 2010

Correspondence to: B. Etzelmüller (bernde@geo.uio.no)

Published by Copernicus Publications on behalf of the European Geosciences Union.

Abstract

Variations in ground thermal conditions in Svalbard were studied based on measurements and theoretical calculations. Ground temperature data was used to calibrate a transient heat flow model describing depth and time variations in temperatures. The model was subsequently forced with historical surface air temperature data records and downscaled global climate model runs to project ground temperatures. We discuss ground temperature development since the early 20th century, and the thermal responses in relation to ground characteristics and snow cover. The modelled ground temperatures show a gradually increase since the end of the Little Ice Age (mid 19th century on Svalbard), by about 1.5 °C to 2 °C at 20 m depth. The active layer thickness (ALT) is modelled to have increased slightly, with the rate of increase depending on water content of the near-surface layers. The used scenario runs predict a significant increase in ground temperatures and an increase of ALT depending on soil characteristics.

1 Background and objectives

Changes in the spatial extent and temperatures of permafrost are generally taken as indications of climate change (e.g. Lachenbruch and Marshall, 1986). Permafrost is continuous in the parts of the high-arctic archipelago Svalbard not covered by glaciers (75–82° N) (e.g. Humlum et al., 2003; Liestøl, 1977). The location of Svalbard in the northern part of the warm North-Atlantic ocean current makes its climate especially sensitive to atmospheric and oceanic changes (e.g. Aagaard and Carmack, 1989). Accordingly, a 4–6 °C warming and +5% precipitation increase are projected by Global Circulation Models (GCM) for Svalbard by 2100 according to the SRES A1b emission scenario (Benestad, 2005; ACIA, 2005). Since permafrost inhibits prominent groundwater flow and stabilizes frozen, unconsolidated sediments, the degradation of permafrost is likely to have wide influences on the processes shaping the physical and

Discussion Paper | Discussion Paper | Discussion Paper | Discussion Paper |

TCD

4, 1877–1908, 2010

Modelling past and future permafrost conditions in Svalbard

B. Etzelmüller et al.

human environment (e.g. Williams and Smith, 1989; French, 1996). Temperature profiles through the permafrost reflect to some extent the history of the ground surface temperature, which, however, is closely coupled to air temperature and snow cover (e.g. Lachenbruch and Marshall, 1986; Goodrich, 1982). A Svalbard ground surface temperature reconstruction, based on a heat conduction inversion model, indicated a warming of the permafrost surface of 1.5 °C ± 0.5 °C over the last 6–8 decades (Isaksen et al., 2000) in the bedrock-dominated site of Janssonhaugen. Between 1999 and 2009 the permafrost has warmed there by 0.9 °C at 20 m depth. Significant warming is detectable down to at least 60 m depth, and the present decadal warming rate at the permafrost surface (c. 2 m depth) are on the order of 0.07° Ca^{-1}, with indications of accelerated warming during the last decade (Isaksen et al., 2007b).

In this paper, we used ground temperatures collected in five boreholes, which were mainly established during the International Polar Year project TSP-Norway (Thermal state of permafrost; Christiansen et al., 2010) to calibrate a 1-D heat conduction model and establish statistical relationships between local ground surface temperatures (GST) and surface air temperature (SAT) at a nearby meteorological station. This framework enables the reconstruction of borehole temperatures since 1912 using a historical record of air temperature. Further, we assess the possible future permafrost conditions and the related uncertainties, by using downscaled air temperature projections from an ensemble of GCMs for the 21st century (Benestad, 2008).

2 Permafrost and air temperature observations

We used four locations studying five boreholes, situated in the central and western part of Spitsbergen, and covering an roughly west-east transect from the most maritime west-coast at Kapp Linné to the inland in the Longyearbyen/Adventdalen area (Fig. 1, Table 1). An overview over location, landforms, stratigraphy and detailed instrumentation of these sites is given by Christiansen et al. (2010). Site information particularly relevant for this study is given below and in Table 1. Three boreholes were drilled in bedrock with little (some cm) sediment cover and thin snow cover (Janssonhaugen, Kapp Linné borehole, BH 1), whereas the other boreholes have a considerable sediment cover consisting of 1 m regolith at Gruvefjellet, a solifluction sheet with 6-7 m diamicton (Endalen) and beach ridge sandy to pebbly sediments at Kapp Linné BH 2. The two boreholes at Kapp Linné are less than 100 m apart from each other, differing only by the amount of sediment cover. At all boreholes ground temperature is recorded automatically, usually in 1 or 6 h intervals, with the longest series from Janssonhaugen (Isaksen et al., 2000). On-site meteorological observations are available from Janssonhaugen, Kapp Linne and Gruvefjellet.

3 Methodology

3.1 Historical meteorological data

West Spitsbergen has three official meteorological stations with longer time series, Svalbard Airport (close to Longyearbyen), Isfjord Radio (Kapp Linné) and Ny-Ålesund (Fig. 1). Mean annual air temperature (MAAT) for the standard normal period 1961–1990 for Svalbard Airport is −6.7 °C, and mean annual precipitation is 190 mm. The Isfjord Radio station shows slightly more maritime conditions, having higher precipitation and means surface air temperature is 1.6 °C higher. The temperature variability is highly correlated between the three stations ($r^2 > 0.9$), with the largest differences between Svalbard Airport and Isfjord Radio. The homogenised monthly temperature series of Svalbard Airport (1912 – present) (Nordli and Kohler, 2004) is a composite of several shorter series of measurements carried out at a few nearby sites (Fig. 2). All shorter series are adjusted to the current Svalbard Airport meteorological station (established in 1975). The beginning of the series coincides with the end of the Little Ice Age in Svalbard (Fig. 2). Since 1912 annual mean temperatures have changed by about 4 °C, from c. −8 °C at the end of the last century to −4 °C today. Temperature varied between −8 °C and −5 °C (Fig. 2) between 1920 and c. 1960. Since the late 1980s

TCD
4, 1877–1908, 2010

MAAT has again increased. The main characteristics of Svalbard's air temperature development since the end of the Little Ice age is the two cold decades in the 1910s and 1960s and the warm spell around the 1930s and the 1950s. Since 1990 a significant positive trend is seen. Inter-annual variations are large, and are mostly driven by variations in winter temperatures, while summer temperatures exhibit little variation. This pattern clearly demonstrate the maritime setting of the archipelago (cf. Førland and Hannssen-Bauer, 2003).

3.2 GCM scenario data for Svalbard Airport

For Svalbard Airport monthly air temperatures covering the 20th and 21st Centuries are available (Fig. 2) based on empirically statistically downscaling an ensemble of GCM scenarios (Benestad, 2008). Large-scale monthly mean surface air temperature (SAT) was used as predictor to derive the local monthly temperature for Svalbard Airport. The calibration of the downscaling models was based on the 40 year reanalysis of the European Centre of Medium-range Weather forecast (ERA40; Uppala et al., 2005) and the station climate archive of the Norwegian Meteorological Institute. The calibration and projection were carried out for each of the calendar months separately, and subsequently assembled for the whole year.

This set of global climate model simulations is from the multi-model World Climate Research Programme (WCRP) Coupled Model Intercomparison Project (CMIP3; Meehl et al., 2007) of the most recent Special Report Emission Scenario (SRES) A1b (in which atmospheric CO_2 reaches 720 ppm by 2100) reported for the Intergovernmental Panel on Climate Change (IPCC) Assessment Report 4 (AR4; Solomon et al., 2007). A common framework of empirical orthogonal functions was used to ensure that similar large-scale spatial patterns in the GCMs as in the ERA40 were used to predict the local temperature for Svalbard Airport (Benestad, 2001).

The Arctic Climate Impact Assessment (ACIA, 2005) provided more detailed analysis on the Arctic, for which an enhanced greenhouse gas warming is expected to be more pronounced than elsewhere on the planet.

TCD
4, 1877–1908, 2010

3.3 Ground temperatures

The ground temperatures in the boreholes vary mainly according to elevation, distance to sea, land form types, and by variations in snow cover and near surface ice- and water content. In the year from summer 2008 to summer 2009, boreholes had mean ground temperatures (MGT) at 15 m depth ranging from −3.2 °C at the west coast at Kapp Linné and in the valley bottom of Endalen to −5.4 °C and c. −6 °C further inland and at higher elevation at Janssonhaugen (Fig. 3e–h). The Endalen borehole has higher ground temperatures, which is related to the snow cover, and moister summer ground conditions due to receiving runoff from upslope areas (Christiansen et al., 2010). The active layer thicknesses (ALT) varied between around 2 m in the bedrock sites of Kapp Linné and Jannsonhaugen to close to 1 m in the Endalen site and Gruvefjellet sites (Christiansen et al., 2010).

On each site ground surface temperature (GST) is measured, either by a separate data logger in c. 5 cm depth or by the first thermistor located at 0 m depth in the borehole. The records from Kapp Linné, Gruvefjellet and Janssonhaugen reveal a relatively close coupling between GST and SAT, while at Endalen, coupling is complicated by more pronounced snow and vegetation covers and their associated insulating properties (Fig. 3d). We calculated the ratios of annual sums of freezing or thawing degree days of GST to those of SAT, referred to as *n*-factors n_T and n_F, respectively (e.g. Smith and Riseborough, 2002). For the non-vegetated sites, the thawing *n*-factor $n_T \geq 1$ (Kapp Linné 1.00, Gruvefjell 1.18, Janssonhaugen 1.13), symptomatic for equal or warmer summer conditions at the ground surface than at screen level (2 m above ground). At the Endalen site, n_T was considerable lower (0.83), equivalent to lower summer GST than summer SAT. The freezing *n*-factor (n_F) depends mainly on snow cover, with $n_F < 1$ indicating a weak coupling between GST and SAT due to the insulating effect of the snow cover. The Endalen site showed lowest n_F with 0.78, while at all the other sites n_F was between 0.95 and 1.

TCD
4, 1877–1908, 2010

These n-factors were then used to derive GST series for each site from the long-term SAT series (1912–2009) and from the multi-model ensemble SAT scenarios (2001–2100) for Svalbard Airport. This was achieved by first adjusting the SAT from Svalbard Airport to the elevation of the considered site utilizing a simple regression to the sites with meteorological information (Kapp Linné, Janssonhaugen, Gruvefjellet), with a $r^2 > 0.9$, or a lapse rate (Endalen). Subsequently, we applied n-factorization. The $r^2 > 0.75$ was achieved for all sites during the calibration period (Fig. 3a–d).

3.4 Heat flow model

The subsurface temperature distribution was simulated by numerically solving the transient 1-D heat equation for non-constant coefficients (see also Farbrot et al., 2007 for more details):

$$\rho\, c \frac{\partial T}{\partial t} = -\frac{\partial}{\partial z}\left(k \frac{\partial T}{\partial z}\right) \tag{1}$$

(Williams and Smith, 1989). As boundary conditions, we prescribe time series of GST and the geothermal heat flux $Q_{geo} = 65\,\mathrm{mW\,m^{-2}}$ at depth. The thermal properties of the ground are described by density ρ, thermal conductivity k and heat capacity c. The presence of water in the substrate has a twofold effect on the thermal properties. First, the thermal properties of water and ice are different to those of the matrix, and we consider effective values as a linear mixture of values for the substrate and the corresponding ones for the volumetric content of water or ice, depending on the temperature conditions. Secondly, the water content affects the thermal properties during the phase transitions. During freezing or thawing, the latent heat associated with these phase changes is released or consumed, respectively. In our model runs, we apply an apparent heat capacity to consider the change of latent heat L due to phase changes of the pore water within a small temperature interval of $\pm 0.1\,^{\circ}\mathrm{C}$ around the freezing temperature (e.g. Wegmann et al., 1998)

$$c_{(T)} = c_0 + \frac{L}{(T_2 - T_1)} \quad (2)$$

Further, any effects of heat advection related to water flow in the active layer are neglected in our modelling. The heat conduction equation (Eq. 1) was discretized along the borehole depth using finite differences and subsequently solved by applying the method of lines.

3.5 Calibration and model initialisation

To achieve a first impression of the parameter space, the mean apparent thermal diffusivity (κ_a) was determined for the different layers at the borehole locations following Williams and Smith (1989):

$$\kappa_a = m^2/p \quad (3)$$

where m is the slope of a linear fit to the natural logarithm of the maximum amplitude $A(z)$ versus depth, assuming that the period p is one year. Effective diffusivities ranged from around 0.7–2.6 × 10^{-7} $m^2 s^{-1}$ in the surface sediment layers to 10–19 × 10^{-7} $m^2 s^{-1}$ in sedimentary bedrock (Table 1).

All borehole models in this study were calibrated to closely reproduce measured ground temperatures (Fig. 4). Each calibration was started from the observed distribution of ground temperatures, at least one month after drilling, when thermal disturbance from the drilling was assumed to be negligible. The model domain was 150 m discretized in constant steps of 0.1 m. For thermal conductivity and bedrock density literature values were used and fine-adjusted during calibration (Table 1). Main calibration parameter was the water content, influencing the effective damping and retardation of the temperature signal. The calibration period was between 500 and 680 days (see Table 1). The calibrated models show good correspondence between observed and modelled temperatures yielding r^2-values of above 0.9 (Fig. 4). However, the Gruvefjellet site is the most weakly constrained one because of coarsely-spaced sensors and lacking information from depth below 5 m.

For Janssonhaugen, ground temperature is measured since May 1998, and local meteorological records are available since spring 2000. At this location we divided the dataset into a calibration (May 2000–May 2005) and a validation period (June 2005–April 2009) (Fig. 4). The model performed well in closely reproducing measured temperature time series at various depths as well as the active layer thickness (Fig. 4).

To reproduce a realistic temperature distribution at depth below the lowermost sensor (Jansonhaugen 100 m, otherwise ~5–40 m), the models were initialised using colder conditions than today. For all boreholes we used SATs derived from the mean MAAT 1912–1922 from Svalbard Airport (–8 °C) and superimpose a harmonic function to mimic the seasonal variation of SAT. The amplitude of that variation was derived from the observed variations of the respective SAT records (typically $r^2 > 0.8$). The models were then spun up over 200 years or until steady state was reached.

4 Results

4.1 Past development

Janssonhaugen is the best calibrated and validated series, as data on deeper ground temperatures is available below 50 m. Our model was forced using site-specific GST series (Fig. 3a–d) which in turn were derived from the instrumental record from Svalbard Airport (Fig. 2). Model results show for all sites a 1–3 °C permafrost temperature increase over the last century at 10 m depth; at 50 m depth ground temperatures have increased by < 1 °C (Fig. 5a–b), and at 100 m depth only minor variations were modelled. The largest changes were modelled at Kapp Linné BH1, presumably because of the assumed low water content and the associated low thermal buffering capacity (Fig. 5). At all sites the modelled ALT shows some inter-annual variation but no clear trend between c. 1920 and c. 1990, later more substantial warming have led to an increase in ALT (Fig. 5c-d). The simulated ALT increase since the 1990s is between 1.25 cm a^{-1} (Gruvefjellet) to 3 cm a^{-1} (Kapp Linné BH1 and Janssonhaugen). For the

TCD
4, 1877–1908, 2010

sediment-rich locations Endalen and Kapp Linné BH2, the change rates in ALT were similar with 1.25 cm a^{-1} and 2.2 cm a^{-1}, respectively (Fig. 5c).

4.2 Future development

All together 32 individual SAT scenarios derived from downscaling a multi-model GCM ensemble were used to further derive GST series for the individual borehole locations, which in turn provided the surface boundary conditions to drive the ground heat conduction models. For Janssonhaugen, the model was initialised from observed January 2000 temperatures, and the others were started from the end of the subsurface temperature reconstruction described above. The uncertainty of the future evolution is demonstrated by the spread of the individual SAT scenarios within the ensemble (Figs. 2 and 6). Here, we present the median of the different results to provide a balanced picture of the potential future development of the ground thermal regime along with the 10% and 90% percentiles to indicate the uncertainty for two of the sites (Figs. 5 and 6). The climate scenario forcing revealed the following major effects of the permafrost thermal state:

1. The expected SAT warming during the 21st century will result in a significant warming in the near-surface layers (Figs. 5 and 6).

2. The spread of the individual scenarios at the depth of zero annual amplitude (ZAA) varies between 5 °C and 2.5 °C, depending on ice/water content and distance to the 0 °C isotherm (Fig. 6).

3. Warming rates are efficiently reduced where the temperature is close to 0 °C and where ice is present due to the consumption of latent heat for

4. The median ground temperatures at the depth of ZAA is suggested to increase by 2–4 °C over the period 2000–2100.

5. Over the same period, ALT increases at all sites, the magnitudes of the modelled increase depend on GST and ground characteristics. While ALT roughly doubles

TCD
4, 1877–1908, 2010

at Gruvefjellet (+0.7 m), Endalen (+1 m), Kapp Linné BH2 (+2.5 m) and Janssonhaugen (+2 m), the increase is more pronounced at Kapp Linné BH1 (+8 m) and may lead to the development of taliks. The spread of ALT for the individual scenarios increases towards the end of the period and depends on assumed water/ice content (Fig. 5c). Apart from Gruvefjellet, taliks develop at all other sites for GST scenarios above the 75% percentile.

6. Model results show degradation of permafrost in bedrock sites at low elevations. Contrarily, at sediment sites with a high water content, modelled ground temperatures increase to close to 0 °C, but permafrost conditions still remain stable until 2100.

7. During 2000 and 2009 we have an overlap between scenario and instrumental data at the Janssonhaugen site. The ALT modelled based on the scenario median slightly overestimates modelled ALT when using observed GSTs (Fig. 5d).

4.3 Sensitivity to changes in temperature

A sensibility analysis was conducted for the study sites, addressing the effect of temperature changes in different seasons. This was achieved by attenuating the amplitudes above and below 0 °C, respectively, of the GST by a factor between 0 and 1, and extracting the associated ground temperature at 15 m depth and the active layer thicknesses (Fig. 7). The results suggest for a given temperature change that an increase of winter temperature and/or increase of snow cover has a major effect on warming the permafrost, while an increase in summer temperature mainly affects the ALT. However, also the warming during winter affects the ALT. The bedrock sites had a more rapid response both with respect to ALT and ground temperature because of a low water content, with especially quick reactions in the Kapp Linné BH1 site.

TCD
4, 1877–1908, 2010

5 Discussion

5.1 Uncertainties and sensitivity

The major uncertainties for this study are related to (1) deficits of the heat conduction model, (2) the spread of the SAT-scenario ensemble and (3) the validity of the statistical relationships between SAT at Svalbard Airport and the GST at the borehole sites.

The heat flow model used in this study does not account for annual or inter-annual variations of water content in the upper layers, like other model approaches do (e.g. Zhang et al., 2003; Burn and Zhang, 2009). However, only few measurements are available that address these effects at the borehole sites, and the model performed well during calibration, even in the ice-rich site of Endalen. This behaviour is probably related to the generally low water content in the relatively coarse sediments above bedrock and pure bedrock at the borehole sites. Over the period 1912–2000, precipitation has increased (Førland and Hanssen-Bauer, 2000, 2003) and a further $\sim$5% increase is expected based on the GCM scenarios (Benestad, 2008; Hanssen-Bauer, 2007). Such an increase in precipitation would furthermore increase the water content of the near-surface, depending on snow re-distribution. However, thicker active layers would release water from thawing of the transient layer (Shur et al., 2005), which is ice-rich. On the other hand, an increase in ALT and thawing of ground ice may decrease the water content. It is obvious that the drying of the active layer may lead to non-linear responses of the thermal regime, typically intensifying the increase in temperature, as already observed in mountain sites in southern Norway (Farbrot et al., 2010; Isaksen et al., 2010). In our study this is demonstrated for the two Kapp Linné sites, which show a different response for the ALT projections due to differences in assumed water content. Thus, our estimates here are considered as rather conservative.

Large uncertainties are related to the spread between the individual SAT scenarios. This spread is about 4–6 °C and is larger than uncertainties related to the heat flow model in terms of water content evolution. We believe, that the median of the resultant temperature distribution is the most reliable indication of future evolution. However, the

TCD
4, 1877–1908, 2010

variability of the individual scenarios contain information about the thermal responses in the ground, reflecting soil properties and moisture conditions. At sites where temperatures approach 0 °C, the spread is reduced due to the consumption of latent heat associated with thawing, e.g. the Endalen site. This is in accordance with observed warming trends recently published e.g. by Romanovsky et al. (2010a) and Smith et al. (2010) from Russia and North America, respectively.

The coupling between SAT at Svalbard Airport and GST at the individual sites depends strongly on snow conditions in terms of snow cover thickness and duration. Here, we have derived GST series from SAT using n-factors, implicitly assuming unchanged snow conditions over the considered period. This may seem somewhat unrealistic given the pronounced warming, especially during winter. A general reduction in snow cover duration would lead to a reduced warming of the ground since the heat loss of the ground would be enhanced during the cold period. Recent studies highlight the effect of snow cover thickness and duration on ground temperatures (e.g. Luetschg et al., 2008), while Engelhardt et al. (2010) showed that differences in the timing of a thick snow cover have a similar influence of ground temperature than different forcing climate scenarios. Recently, Christiansen et al. (2010) and Romanovsky et al. (2010b) demonstrated the large differences of near-surface ground temperatures between two adjacent boreholes with different snow cover in Svalbard. Deeper ground temperatures in turn will tend to be similar because of lateral heat transfer. In our study, however, the values of the n_F-factors are close to 1 besides for the Endalen site, indicating little influence of snow on the SAT-GST coupling. Further, the anticipated warming trend would change vegetation towards a larger abundance of higher plants like bushes and thereby alter n_T-factors. Those plants are known to trap snow, potentially increasing the GST during winter considerably, even if summer temperatures would decrease somewhat because of increased shading (e.g. Blok et al., 2010; Sharkhuu et al., 2007; Hinzman et al., 2005).

Finally, the SAT-GST relationships employed here assume a constant lapse rate between Svalbard Airport and the study sites. However, lapse rates are not constant over time and especially at arctic sites highly depending on sea ice conditions and the general circulation pattern. Svalbard Airport is situated close to the coast, and its temperature especially during winter covaries with sea ice cover. The Svalbard Airport is highly sensitive to the coupled sea ice-ocean-atmosphere system (Benestad et al., 2002) and recently observed shrinkage in Arctic sea-ice cover (Vinje, 2001; Stroeve et al., 2007) suggests that larger differences may be expected further inland e.g. at Endalen, Gruvefjellet and Janssonhaugen today than previously (O. Humlum, personal communication, 2010).

In summary, different uncertainties draw in different directions, and the importance of each factor is difficult to quantify or even unknown. We believe, however, that our results provide a fairly realistic picture of consequences of future CO_2-emissions as specified in the A1b scenario.

5.2 Trends and consequences

According to the model the warming since the start of the last century has resulted in a low-gradient temperature profile, which corresponds well with the measured values. We model a c. +0.5 °C difference between modelled and measured GT at 20 m depth for the Janssonhaugen site, while the overall gradient fits well. The offset is probably due to two main reasons. First, the initial temperature distribution is somewhat speculative and temperature may have been too low, as the former ground temperature history is not known. Secondly, lapse rates may have differed during earlier parts of the last century as mentioned above. For all sites the modelled active layer thicknesses correspond to the measured values from the boreholes within c. ± 0.3 m.

During the last 100 years only minor changes occurred in the modelled ground temperatures, apart from the period since the mid 1990s which were the warmest since the instrumental record started. The last 10–15 years warming can explain almost 50% of the simulated warming in the uppermost 50 m of the permafrost. We clearly see the warm year of 2006/2007, described and analysed in Isaksen et al. (2007a), with a considerable increase in ALT at all sites apart from Gruvefjellet. Individual warm events like that in spring 2006 are important, as the system needs time to recover, as e.g. demonstrated for the Alps after a similar event in 2003 (c.f. Hilbich et al., 2008; Gruber et al., 2004). In general, the active layer change during the recent years, and especially during the last decades is similar to observations in other parts of the world (Romanovsky et al., 2010a; Smith et al., 2010; Zhao et al., 2010; Christiansen et al., 2010).

In Svalbard the temperature variability during summer and winter is different. While summer temperatures are fairly constant between years, the variability of winter temperature is high (Førland et al., 2009). The trends for the entire instrumental SAT record at Svalbard Airport (1912–2009) show that temperatures have increased significantly during spring (MAM, $+0.044^{\circ}\,\mathrm{C}\,\mathrm{a}^{-1}$), winter (DJF, $+0.015^{\circ}\,\mathrm{C}\,\mathrm{a}^{-1}$) and autumn (SON, $+0.014^{\circ}\,\mathrm{C}\,\mathrm{a}^{-1}$), whereas summer (JJA, $+0.009^{\circ}\,\mathrm{C}\,\mathrm{a}^{-1}$) temperatures were more constant during the last century (Førland et al., 2009). Our sensitivity study suggests that the increase of winter temperatures leads to a substantial warming of the permafrost, while the relatively constant summer temperatures have only a minor influence and mainly on the active layer thickness. An exception is the bedrock site at Kapp Linné BH1, which shows a somewhat faster response also in ALT when winter temperature increases. This explains the low variability of the modelled ALT during large parts of the last century.

For the future development, the ground thermal regime stays relatively stable for reasons discussed above. However, sites close to sea level are modelled to undergo permafrost degradation and to develop taliks. The major effect is the warming of the permafrost, where temperature are modelled to rise to above −2 °C at 20 m depth in the more continental sites and above −1 °C at the lower sites like Endalen and Kapp Linné. Such temperature conditions are currently observed within the discontinuous mountain permafrost in e.g. the high mountains of the Norwegian mainland (Christiansen et al., 2010; Farbrot et al., 2010).

Major permafrost changes are mainly to be expected by the end of the 21st century along the coast lines and in the outer parts of the large glacial valleys of

Nordenskiöldland (Fig. 8) below 100 m a.s.l., where the permafrost is warmest and where the local settlements are located. These areas are characterized by the presence of mainly marine, raised beach sediments, fluvial and glaciofluvial sediments, partly overlain by eolian, colluvial or alluvial deposits, having a relatively fine matrix (Christiansen et al., 2010). Those sediments are ice-rich, and associated periglacial landforms such as ice wedges, pingos and solifluction sheets or lobes are wide-spread (Christiansen, 2005; Harris et al., 2009; Ross et al., 2007). Addressing the consequences of climate change on certain periglacial processes remains a challenge. The possible thaw of the ice-rich layers in the transitions zone on the top of permafrost has received considerable attention (Büdel, 1982; Shur et al., 2005; Murton et al., 2006). On one hand, this effects buffers ground warming, on the other hand it may cause a non-linear response if completely thawed. Resulting increases in ALT may in certain areas of Svalbard be associated with unprecedented thaw settlement as ice-rich soils if the upper permafrost layer thaws (Nelson et al., 2001), and in consequence, a marked increase in slope instability (Harris et al., 2001, 2009; Davis et al., 2001; Gruber and Haeberli, 2007). An important geomorphological consequence for bedrock in coastal areas is coastal erosion. The coastal sections within the study areas have a large frequency of rock cliffs (e.g. Etzelmüller et al., 2003; Ødegård et al., 1987) formed in sedimentary bedrock. Those are heavily shattered by frost weathering, and probably an important source for material transport and erosion into the sea (e.g. Ødegård et al., 1995; Ødegård and Sollid, 1993). Such sites would be highly susceptible to proposed changes, supposing that many cliffs are stabilized by permafrost.

6 Conclusions

From this study the following conclusions are drawn:

- The substantial warming of ground temperatures and associated active layer thickening observed in recent years on Janssonhaugen was successfully reproduced by our model.

TCD
4, 1877–1908, 2010

- Since the end of the Little Ice Age on Svalbard (mid to end of 19th century) and until 1990, permafrost has warmed up by around 1 °C and since then by 0.5–1 °C. There was little variation in modelled ALT over these 100 years although there was substantial variability of air temperature. MAAT changes were mainly caused by the increase of winter temperatures and thus have less influence on ALT.

- A similar pattern is valid for future development, with a general warming of permafrost, but limited changes in ALT at least at ice-rich sites.

- The sensitivity analysis shows that GT is more sensitive to changes in winter temperatures than to changes in summer temperatures for sites with sediment cover. Changes in summer temperatures have a direct impact on ALT whereas ALT is only indirectly affected by changes in winter temperatures through the general influence on GT.

- Permafrost degradation can be expected at low elevation, e.g. close to the coast below c. 100 m a.s.l. in well-drained and dry sites (e.g. bedrock), where the development of taliks is likely. From this analysis a major degradation of permafrost is not expected on Svalbard during the next c. 50 years for areas with no ground disturbances by human activity.

Acknowledgements. This study was funded and supported by the Norwegian Research Council, project no. 176033/S30 (Permafrost Observatory Project: a Contribution to the Thermal State of Permafrost in Norway and Svalbard) and 185987/V30 (CRYOLINK – Permafrost and seasonal frost in Southern Norway: understanding and modelling the atmosphere-ground temperature), the University of Oslo, Norway, the University Centre of Svalbard (UNIS), the Norwegian Meteorological Institute, Oslo, and the Geological Survey of Norway, Trondheim. We want to thank all mentioned institutions.

TCD
4, 1877–1908, 2010

References

Aagaard, K. and Carmack, E. C.: The Role of Sea Ice and Other Fresh-Water in the Arctic Circulation, J. Geophys. Res.-Oceans, 94, 14485–14498, 1989.

ACIA: Arctic Climate Impact Assessment, Cambridge University Press, Cambridge, UK, 1042 pp., 2005.

Benestad, R. E.: A comparison between two empirical downscaling strategies, Int. J. Climatol., 21, 1645–1668, 2001.

Benestad, R. E., Førland, E. J., and Hannssen-Bauer, I.: Empirically downscaled temperature scenarios for Svalbard, Atmos. Sci. Lett., 3, 71–93, 2002.

Benestad, R. E.: Climate change scenarios for northern Europe from multi-model IPCC AR4 climate simulations, Geophys. Res. Lett., 32, L17704, doi:10.1029/2005gl023401, 2005.

Benestad, R. E.: Empirical-Statistical downscaled Arctic Temperature and precipitation, Series, Met. no Report 12/2008 Climate, Norwegian Meteorological Institute, Oslo, 2008.

Blok, D., Heijmans, M. M. P. D., Schaepman-Strub, G., Kononov, A. V., Maximov, T. C., and Berendse, F.: Shrub expansion may reduce summer permafrost thaw in Siberian tundra, Global Change Biol., 16, 1296–1305, 2010.

Burn, C. R. and Zhang, Y.: Permafrost and climate change at Herschel Island (Qikiqtaruq), Yukon Territory, Canada, J. Geophys. Res.-Earth, 114, F02001, doi:10.1029/2008JF001087, 2009.

Büdel, J.: Climatic Geomorphology, Princeton University Press, Princeton, 443 pp., 1982.

Christiansen, H. H.: Thermal regime of ice-wedge cracking in Adventdalen, Svalbard, Permafrost Periglac., 16, 87–98, 2005.

Christiansen, H. H., Etzelmuller, B., Isaksen, K., Juliussen, H., Farbrot, H., Humlum, O., Johansson, M., Ingeman-Nielsen, T., Kristensen, L., Hjort, J., Holmlund, P., Sannel, A. B. K., Sigsgaard, C., Akerman, H. J., Foged, N., Blikra, L. H., Pernosky, M. A., and Odegard, R. S.: The Thermal State of Permafrost in the Nordic Area during the International Polar Year 2007–2009, Permafrost Periglac., 21, 156–181, doi:10.1002/Ppp.687, 2010.

Davis, M. C. R., Hamza, O., and Harris, C.: The effect of rise in mean annual temperature on the stability of rock slopess containing ice-filled discontinuities, Permafrost Periglac., 12, 137–144, 2001.

Engelhardt, M., Hauck, C., and Salzmann, N.: Influence of atmospheric forcing parameters on modelled mountain permafrost evolution, Meteorol. Z., in press, 19(5), 2010.

Etzelmüller, B., Ødegård, R. S., and Sollid, J. L.: The spatial distribution of coast types on Svalbard, in: Arctic Coastal Dynamics – Reports of the 3rd International Workshop, University of Oslo (Norway), 2–5 December 2002, edited by: Rachold, V., Brown, J., Solomon, S., and Sollid, J. L., Reports on Polar and Marine Research, Alfred Wegener Institute for Polar and Marine Research, Bremerhaven, 33–40, 2003.

Farbrot, H., Etzelmüller, B., Gudmundsson, A., Schuler, T. V., Eiken, T., Humlum, O., and Björnsson, H.: Thermal characteristics and impact of climate change on mountain permafrost in Iceland, J. Geophys. Res., 112, F03S90, doi:10.1029/2006JF000541, 2007.

Farbrot, H., Etzelmuller, B., Hipp, T., Isaksen, K., Ødegård, R. S., and Humlum, O.: Air and ground temperatures along elevation and continental gradients in Southern Norway, Permafrost Periglac., in review, 2010.

French, H. M.: The periglacial environment, 2nd edition, Longmann, London, 341 pp., 1996.

Førland, E. J. and Hanssen-Bauer, I.: Increased precipitation in the Norwegian Arctic: True or false?, Climatic Change, 46, 485–509, 2000.

Førland, E. J. and Hannssen-Bauer, I.: Past and future climate variations in the Norwegian Arctic: overview and novel analyses, Polar Res., 22, 113–124, 2003.

Førland, E. J., Benestad, R. E., Flatøy, F., Hanssen-Bauer, I., Haugen, J. E., Isaksen, K., Sorteberg, A., and Aadlandsvik, B.: Climate development in North Norway and the Svalbard region during 1900–2100, Norwegian Polar Institute, Tromsø, 44, 2009.

Goodrich, L. E.: The influence of snow cover on the ground thermal regime, Can. Geotech. J., 19, 421–432, 1982.

Gruber, S., Hoelzle, M., and Haeberli, W.: Permafrost thaw and destabilization of Alpine rock walls in the hot summer of 2003, Geophys. Res. Lett., 31, L13504, doi:10.1029/2004gl020051, 2004.

Gruber, S. and Haeberli, W.: Permafrost in steep bedrock slopes and its temperature-related destabilization following climate change, J. Geophys. Res.-Earth, 112, F02s18, doi:10.1029/2006jf000547, 2007.

Hanssen-Bauer, I. and Førland, E. J.: Long-term trends in precipitation and temperature in the Norwegian Arctic: can they be explained by changes in atmospheric circulation patterns?, Climate Res., 10, 143–153, 1998.

Hanssen-Bauer, I.: Climate variation in the European sector of the Arctic: Observations and scenarios, in: Arctic-Alpine Ecosystems and people in a Changing Environment, edited by: Orb, J. B. E. A., Springer Verlag, Hamburg, 2007.

Harris, C., Davis, M., and Etzelmüller, B.: The Assessment of Potential Geotechnical Hazard Associated With Mountain Permafrost in a Warming Global Climate, Permafrost Periglac., 12, 145–156, 2001.

Harris, C., Arenson, L. U., Christiansen, H. H., Etzelmuller, B., Frauenfelder, R., Gruber, S., Haeberli, W., Hauck, C., Holzle, M., Humlum, O., Isaksen, K., Kaab, A., Kern-Lutschg, M. A., Lehning, M., Matsuoka, N., Murton, J. B., Nozli, J., Phillips, M., Ross, N., Seppala, M., Springman, S. M., and Muhll, D. V.: Permafrost and climate in Europe: Monitoring and modelling thermal, geomorphological and geotechnical responses, Earth-Sci. Rev., 92, 117–171, doi:10.1016/j.earscirev.2008.12.002, 2009.

Hilbich, C., Hauck, C., Hoelzle, M., Scherler, M., Schudel, L., Voelksch, I., Muehll, D. V., and Maeusbacher, R.: Monitoring mountain permafrost evolution using electrical resistivity tomography: A 7-year study of seasonal, annual, and long-term variations at Schilthorn, Swiss Alps, J. Geophys. Res.-Earth, 113(F1), F01S90, doi:10.1029/2007JF000799, 2008.

Hinzman, L. D., Bettez, N. D., Bolton, W. R., Chapin, F. S., Dyurgerov, M. B., Fastie, C. L., Griffith, B., Hollister, R. D., Hope, A., Huntington, H. P., Jensen, A. M., Jia, G. J., Jorgenson, T., Kane, D. L., Klein, D. R., Kofinas, G., Lynch, A. H., Lloyd, A. H., McGuire, A. D., Nelson, F. E., Oechel, W. C., Osterkamp, T. E., Racine, C. H., Romanovsky, V. E., Stone, R. S., Stow, D. A., Sturm, M., Tweedie, C. E., Vourlitis, G. L., Walker, M. D., Walker, D. A., Webber, P. J., Welker, J. M., Winker, K., and Yoshikawa, K.: Evidence and implications of recent climate change in northern Alaska and other arctic regions, Climatic Change, 72, 251–298, 2005.

Humlum, O., Instanes, A., and Sollid, J. L.: Permafrost in Svalbard: a review of research history, climatic background and engineering challenges, Polar Res., 22, 191–215, 2003.

Isaksen, K., Vonder Mühll, D., Gubler, H., Kohl, T., and Sollid, J. L.: Ground surface temperature reconstruction based on data from a deep borehole in permafrost at Janssonhaugen, Svalbard, Ann. Glaciol., 31, 287–294, 2000.

Isaksen, K., Benestad, L. E., Harris, C., and Sollid, J. L.: Recent extreme near-surface permafrost temperatures on Svalbard in relation to future climate scenarios, Geophys. Res. Lett., 34, L17502, doi:10.1029/2007GL031002, 2007a.

Isaksen, K., Sollid, J. L., Holmlund, P., and Harris, C.: Recent warming of mountain permafrost in Svalbard and Scandinavia, J. Geophys. Res.-Earth, 112(F2), F02S04, doi:10.1029/2006JF000522, 2007b.

Isaksen, K., Ødegård, R. S., Etzelmuller, B., Hilbich, C., Hauck, C., Farbrot, H., Eiken, T., Hygen, H. O., and Hipp, T.: Degrading mountain permafrost in southern Norway – spatial

and temporal variability of mean ground temperatures 1999–2009, Permafrost Periglac., accepted, 2010.
Juliussen, H., Christiansen, H. H., Strand, G. S., Iversen, S., Midttømme, K., and Rønning, J. S.: NORPERM, the Norwegian Permafrost Database – a TSP NORWAY IPY legacy, Earth Syst. Sci. Data Discuss., 3, 27–54, 2010, http://www.earth-syst-sci-data-discuss.net/3/27/2010/.
Lachenbruch, A. H. and Marshall, B. V.: Changing climate: geothermal evidence from permafrost in the Alaskan Arctic., Science, 234, 689–696, 1986.
Liestøl, O.: Pingos, springs, and permafrost in Spitsbergen, Norsk Polarinstitutt Årbok, 1975, 7–29, 1977.
Luetschg, M., Lehning, M., and Haeberli, W.: A sensitivity study of factors influencing warm/thin permafrost in the Swiss Alps, J. Glaciol., 54, 696–704, 2008.
Meehl, G. A., Covey, C., Delworth, T., Latif, M., McAvaney, B., Mitchell, J. F. B., Stouffer, R. J., and Taylor, K. E.: The WCRP CMIP3 multimodel dataset – A new era in climate change research, B. Am. Meteorol. Soc., 88, 1383, doi:10.1175/Bams-88-9-1383, 2007.
Murton, J. B., Peterson, R., and Ozouf, J. C.: Bedrock fracture by ice segregation in cold regions, Science, 314, 1127–1129, 2006.
Nelson, F. E., Anisimov, O. A., and Shiklomanov, N. I.: Subsidence risk from thawing permafrost – The threat to man-made structures across regions in the far north can be monitored, Nature, 410, 889–890, 2001.
Nordli, Ø. and Kohler, J.: The early 20th century warming, Daily observations at Grønfjorden and Longyearbyen on Spitsbergen, 2nd edition, Norwegian Meteorlogical Institute, Oslo, 2004.
Ødegård, R. and Sollid, J. L.: Coastal cliff temperatures related to the potential for cryogenic weathering processes, western Spitsbergen, Svalbard, Polar Res., 12, 95–106, 1993.
Ødegård, R., Etzelmüller, B., Vatne, G., and Sollid, J. L.: Near-surface spring temperatures in an Arctic coastal rock cliff: Possible implications for rock breakdown, in: Steepland Geomorphology, edited by: Slaymaker, O., Wiley, Chichester, 89–102, 1995.
Ødegård, R. S., Sollid, J. L., and Trollvik, J. A.: Kystkart Svalbard A3 Forlandsundet 1:200 000, Norsk Polarinstitutt and Unviersity of Oslo, Oslo, 1987.
Romanovsky, V. E., Drozdov, D. S., Oberman, N. G., Malkova, G. V., Kholodov, A. L., Marchenko, S. S., Moskalenko, N. G., Sergeev, D. O., Ukraintseva, N. G., Abramov, A. A., and Vasiliev, A. A.: Thermal state of permafrost in Russia, Permafrost Periglac., 22, 136–

TCD
4, 1877–1908, 2010

Modelling past and future permafrost conditions in Svalbard

B. Etzelmüller et al.

155, 2010a.
Romanovsky, V. E., Smith, S. L., and Christiansen, H. H.: Permafrost Thermal State in the Polar Northern Hemisphere during the International Polar Year 2007–2009: a Synthesis, Permafrost Periglac, 21, 106–116, doi:10.1002/Ppp.689, 2010b.
Ross, N., Brabham, P. J., Harris, C., and Christiansen, H. H.: Internal structure of open system pingos, Adventdalen, Svalbard: The use of resistivity tomography to assess ground-ice conditions, J. Environ. Eng. Geoph., 12, 113–126, 2007.
Sharkhuu, A., Sharkhuu, N., Etzelmüller, B., Heggem, E. S. F., Nelson, F. E., Shiklomanov, N., Goulden, C., and Brown, J.: Permafrost Monitoring in the Hovsgol Mountain Region, Mongolia, J. Geophys. Res., 112(F2), F02S06, doi:10.1029/2006JF000543, 2007.
Shur, Y., Hinkel, K. M., and Nelson, F. E.: The transient layer: Implications for geocryology and climate-change science, Permafrost Periglac., 16, 5–17, 2005.
Smith, M. W. and Riseborough, D. W.: Climate and the limits of permafrost: A zonal analysis, Permafrost Periglac., 13, 1–15, 2002.
Smith, S. L., Romanovsky, V. E., Lewkowicz, A. G., Burn, C. R., Allard, M., Clow, G. D., Yoshikawa, K., and Throop, J.: Thermal state of permafrost in North America – a contribution to the International Polar Year, Permafrost Periglac., 22, 117–135, 2010.
Solomon, S., Quin, D., Manning, M., Chen, Z., Marquis, M., Averyt, K. B., Tignotr, M., and Miller, H. L.: Climate Change: The Physical Science Basis. Contribution of Working Group I to the Fourth Assessment Report of the Intergovernmental Panel on Climate Change, Cambridge University Press, UK and New York, NY, USA, 2007.
Stroeve, J., Holland, M. M., Meier, W., Scambos, T., and Serreze, M.: Arctic sea ice decline: Faster than forecast, Geophys. Res. Lett., 34(9), L09501, doi:10.1029/2007GL029703, 2007.
Tolgensbakk, J., Sørbel, L., and Høgvard, K.: Geomorphological and quarternary geological map 1:100 000 Sheet C9Gq Adventdalen, Nor. Polarinst. Temakart, 32, 2000.
Uppala, S. M., Kallberg, P. W., Simmons, A. J., Andrae, U., Bechtold, V. D., Fiorino, M., Gibson, J. K., Haseler, J., Hernandez, A., Kelly, G. A., Li, X., Onogi, K., Saarinen, S., Sokka, N., Allan, R. P., Andersson, E., Arpe, K., Balmaseda, M. A., Beljaars, A. C. M., Van De Berg, L., Bidlot, J., Bormann, N., Caires, S., Chevallier, F., Dethof, A., Dragosavac, M., Fisher, M., Fuentes, M., Hagemann, S., Holm, E., Hoskins, B. J., Isaksen, L., Janssen, P. A. E. M., Jenne, R., McNally, A. P., Mahfouf, J. F., Morcrette, J. J., Rayner, N. A., Saunders, R. W., Simon, P., Sterl, A., Trenberth, K. E., Untch, A., Vasiljevic, D., Viterbo, P., and Woollen, J.:

TCD
4, 1877–1908, 2010

Modelling past and future permafrost conditions in Svalbard

B. Etzelmüller et al.

The ERA-40 re-analysis, Q. J. Roy. Meteor. Soc., 131, 2961–3012, 2005.
Vinje, T.: Anomalies and trends of sea-ice extent and atmospheric circulation in the Nordic Seas during the period 1864–1998, J. Climate, 14, 255–267, 2001.
Wegmann, M., Gudmundsson, G. H., and Haeberli, W.: Permafrost changes in rock walls and the retreat of alpine glaciers: A thermal modelling approach, Permafrost Periglac., 9, 23–33, 1998.
Williams, P. J. and Smith, M. W.: The Frozen Earth: Fundamentals of geocryology, Cambridge University press, Cambridge, 300 pp., 1989.
Zhang, Y., Chen, W. J., and Cihlar, J.: A process-based model for quantifying the impact of climate change on permafrost thermal regimes, J. Geophys. Res.-Atmos., 108, doi:10.1029/2002JD003354, 2003.
Zhao, L., Wu, Q., Marchengo, S., and Sharkhuu, N.: Thermal state of permafrost and active layer in Central Asia during the International Polar Year, Permafrost Periglac., 22, 198–207, 2010.

Discussion Paper | Discussion Paper | Discussion Paper | Discussion Paper |

TCD

4, 1877–1908, 2010

Modelling past and future permafrost conditions in Svalbard

B. Etzelmüller et al.

Table 1. Calibration parameters used for ground temperature modelling

Borehole name and elevation	Layers (lower boundary) m	Thermal conduc. $Wm^{-1}K^{-1}$	Density $kg\,m^{-3}$	Effective diffusivity $m^2\,s^{-1}$	Water content vol %	Ground thermal heat flow Wm^{-2}	Calibration (validation in curs.) time period	Total depth of boreh. m	Stratigraphy	Bedrock type	Logger info
Endalen (53 m a.s.l.)	< 1 2 4 7 > 7	1.0 1.2 1.5 1.7 2.2	1500 1600 1800 2000 2300	1.17×10^{-7} 10×10^{-7} 9.8×10^{-7}	9 12 7 5 3	0.065	17 Sep 2008– 10 Feb 2010	20	Solifluction sheet (c. 5–7 m), weathered bedrock (c. 2 m) (diamicton, inter-layered with finer material, scattered blocks)	Sandstones, siltstones and shale (Middle Jurassic)	YSI 44006 thermistors (± 0.02 °C) Campbell logger
Gruvefjellet (464 m a.s.l.)	< 0.8 1.4 2.4 4 > 4	1.0 1.2 1.3 1.9 2.1	1300 1500 1900 2100 2300	0.7×10^{-7} 14×10^{-7}	5 12 8 4 3	0.065	15 Mar 2008– 10 Feb 2010	5	Regolith (0.8 m)	Sandstones, shale (Palaeocene to Eocene-Tertiary)	Campbell logger, RST (c) thermistor (± 0.1 °C)
Kapp Linné BH1 (10 m a.s.l.)	< 3 6 10 14 > 14	2 2.5 2 2.8 2.8	2200 2300 2700 2700 2700	2.6×10^{-7} 19×10^{-7} 24×10^{-7}	3.5 2.5 1.5 1 1	0.065	23. Sep 2008– 18. Mar 2010	30	Bedrock	Schist and carbonates (pre-Devonian)	YSI 44006 thermistors (± 0.02 °C) Campbell logger
Kapp Linné BH2 (10 m a.s.l.)	< 2 5 6.5 15 > 15	0.6 1.5 1.2 2.6 2.8	1000 1500 1200 2500 2700	1.4×10^{-7} 7.8×10^{-7} 12×10^{-7}	1.5 9 3 2 2	0.065	23 Sep 2008– 18 Mar 2010	40	Litoral beach ridge sediments (6–7 m) (2 m pebbles 2.5 m sand/silt 1.5 m pebbles)	Shiest and carbonates (pre-Devonian)	YSI 44006 thermistors (± 0.02 °C) Campbell logger
Jansson -haugen (270 m a.s.l.)	< 1 3 > 3	1.6 1.8 2.2	2300 2300 2300	2.1×10^{-7} 9.3×10^{-7} (...)	6 5 3	0.065	1 Jan 2000– 21 Dec 2004 1 Jan 2005– 27 Feb 2009	102	Bedrock	Sandstone, with some thin layers of shale (Middle Jurasic)	YSI 44006 thermistors (± 0.02 °C) Campbell logger

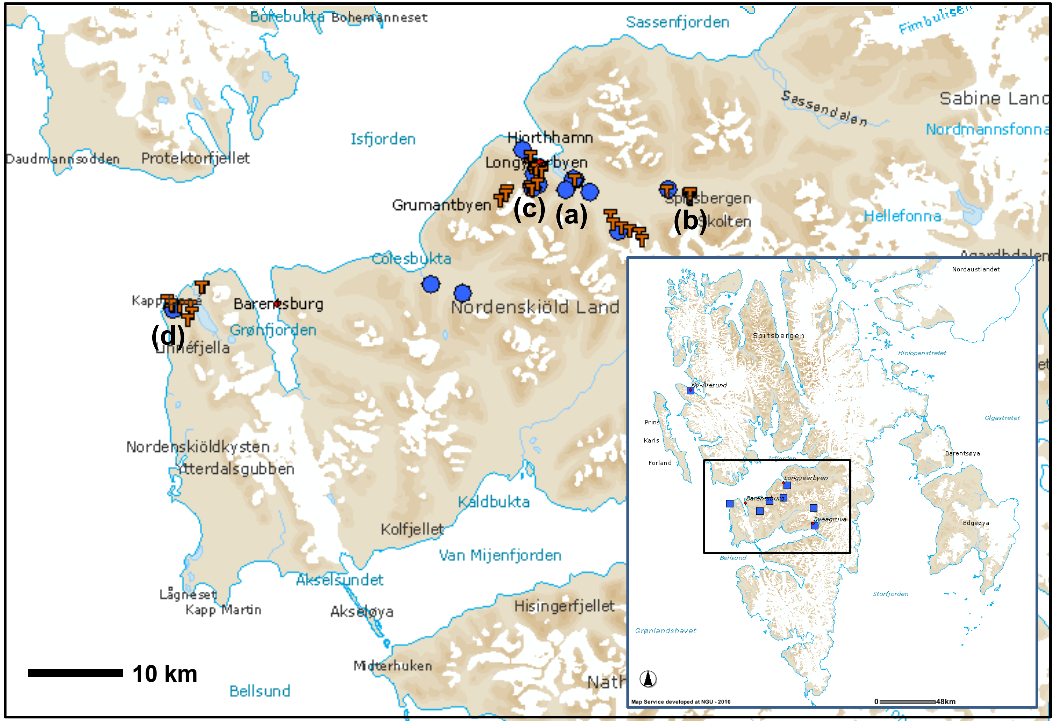

Fig. 1. Location of the studied borehole sites in Svalbard in the Nordenskiöldland Permafrost Observatory (Juliussen et al., 2010). The selected sites for this study on Nordenskiöld peninsula are Endalen **(a)**, Janssonhaugen **(b)**, Gruvefjellet **(c)** and Kapp Linné **(d)**. The blue circles show borehole location, while the "*T*"s indicate locations for ground surface temperature monitoring. The blue boxes in the inlet map are defined permafrost regions on Svalbard, where monitoring is carried out.

TCD

4, 1877–1908, 2010

Modelling past and future permafrost conditions in Svalbard

B. Etzelmüller et al.

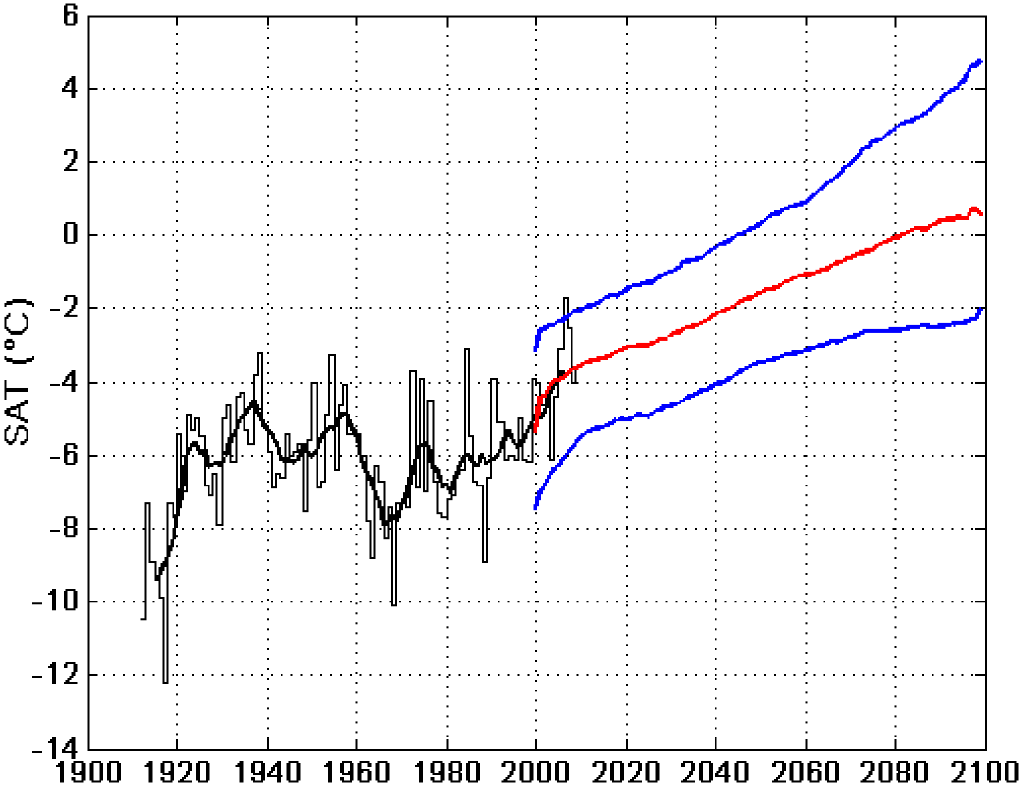

Fig. 2. The official mean annual surface air temperature record at Svalbard Airport. The bold line represents a 7 year Gauss-filtered series of MAAT with three standard deviations. The distribution of the 32 downscaled future scenarios are displayed as percentiles between 2000 and 2100, where the red line is the median and the blue lines represent the 10% and 90% percentiles, respectively. Note that the observed annual temperature closely matches the scenario median in the 10 year overlap period, with the extreme year of 2006/2007 being outside even the 90% percentile (Isaksen et al., 2007a).

TCD
4, 1877–1908, 2010

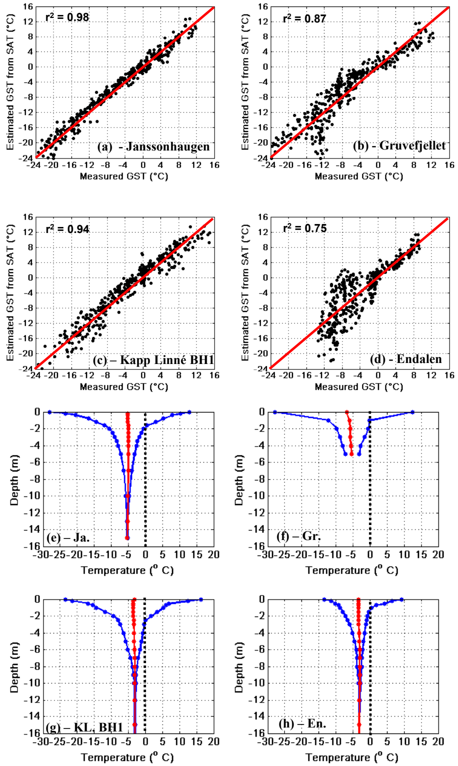

Fig. 3. (a–d) Measured ground surface temperature (GST) plotted against estimated GST based on the surface air temperature (SAT) from Svalbard Airport and a *n*-factor based transfer function. Only the Endalen site showed a significant effect of snow cover during winter, resulting in a lower but still satisfying r^2 of above 0.75. At the other sites, modelled and observed GST agree well ($r^2 > 0.87$). **(e–h)** The red lines represent measured mean ground temperature at various depth for the 2008/2009 period. The envelope of maximum and minimum temperatures is shown by the blue lines. Thermistor locations are indicated by the solid circles.

TCD
4, 1877–1908, 2010

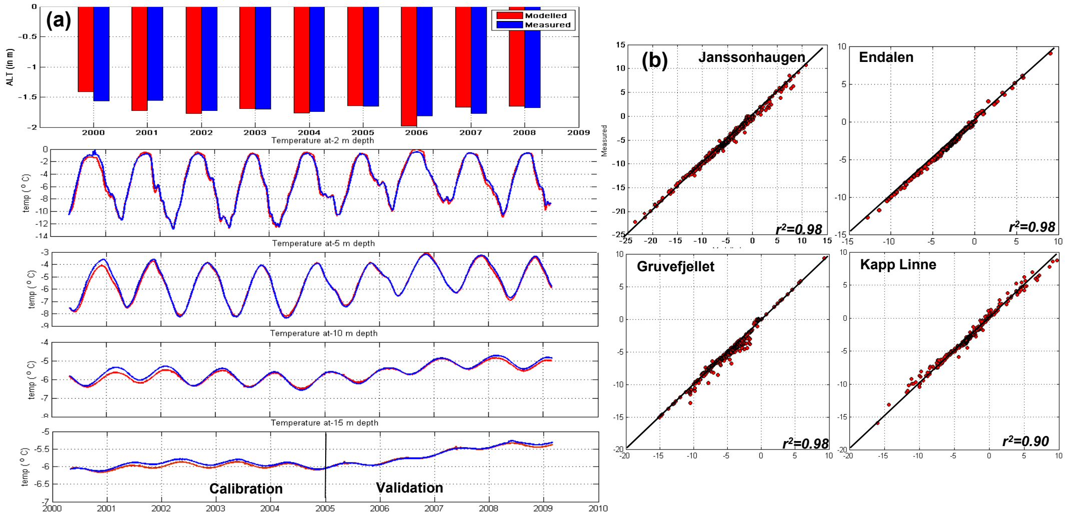

Fig. 4. (a) Calibration and validation plots for Janssonhaugen, comparing active layer thickness (ALT, upper) and temperature development in different depths (lower). **(b)** Scatter plots between measured and modelled ground temperatures at the various study sites.

TCD
4, 1877–1908, 2010

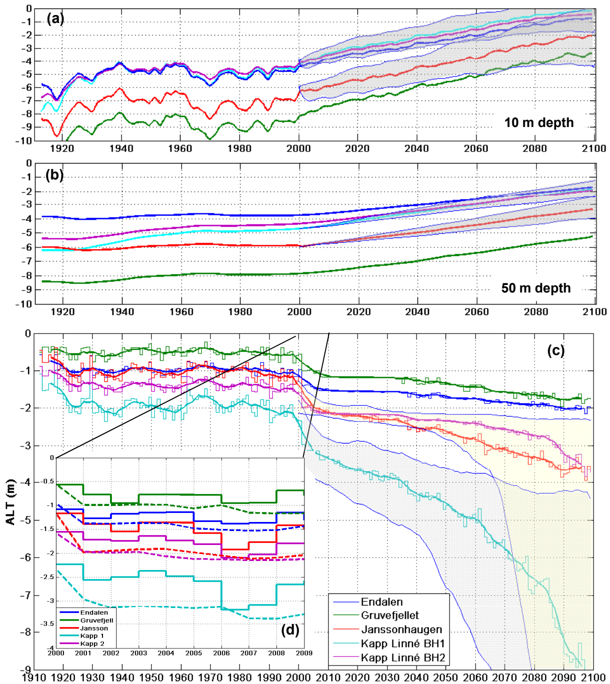

Fig. 5. Evolution of ground temperatures and ALT 1912–2099. Until 2000 the model was driven by instrumental data, from 2000 results of the scenario runs are shown.. All series were smoothed with a 24 months Gaussian filter with three standard deviations. **(a)** Ground temperature development since 1912 in 10 m and **(b)** 50 m depth. The shaded areas illustrate the spread of model results between the 10% and 90% percentiles. The shaded area is only given for the Kapp Linné BH1 and Janssonhaugen site. **(c)** Modelled maximum active layer thickness during the same period. The shaded area illustrates the modelled ALT spread for the 10% and 90% percentile scenario results for the Kapp L. BH1 site (gray, bedrock site) and the Kapp L. BH2 (yellow, sediment-covered site). **(d)** Comparison between modelled ALT based on instrumental data (solid line) and median GCM scenario run (stippled line) in the overlap period 2000–2010.

TCD
4, 1877–1908, 2010

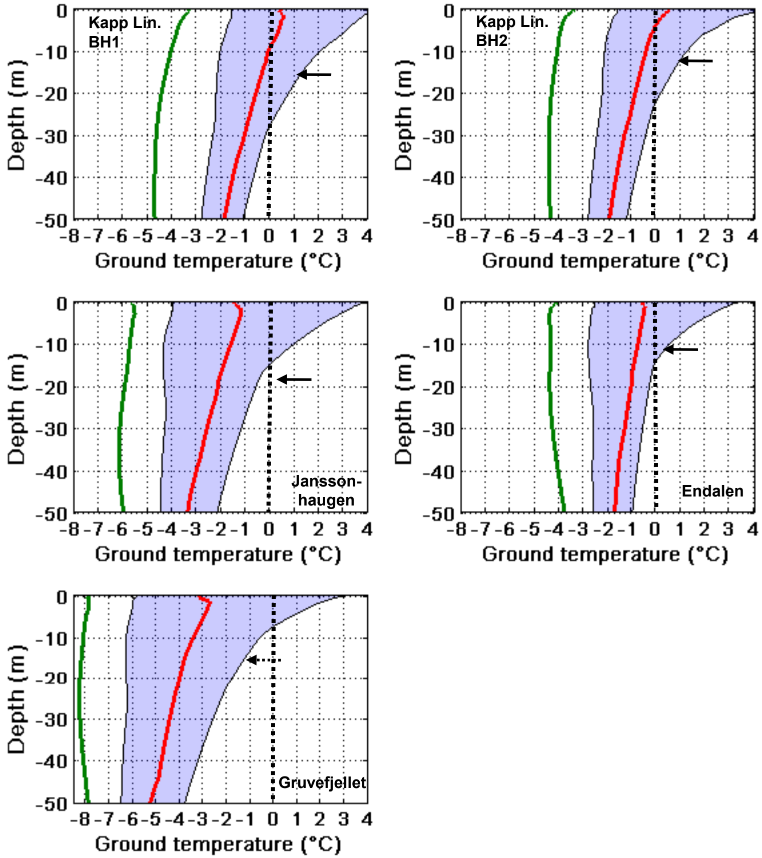

Fig. 6. Predicted future evolution of permafrost temperatures. The green lines represent the start conditions, either measured (Janssonhaugen) or derived from the historic modelling based on instrumental data from JAN/2000 (all other sites). The red line is the median of all scenario results, the shaded polygon denotes minimum and maximum GT from the scenario runs. The ZAA is indicated by an arrow and is situated between 10 and 20 depth.

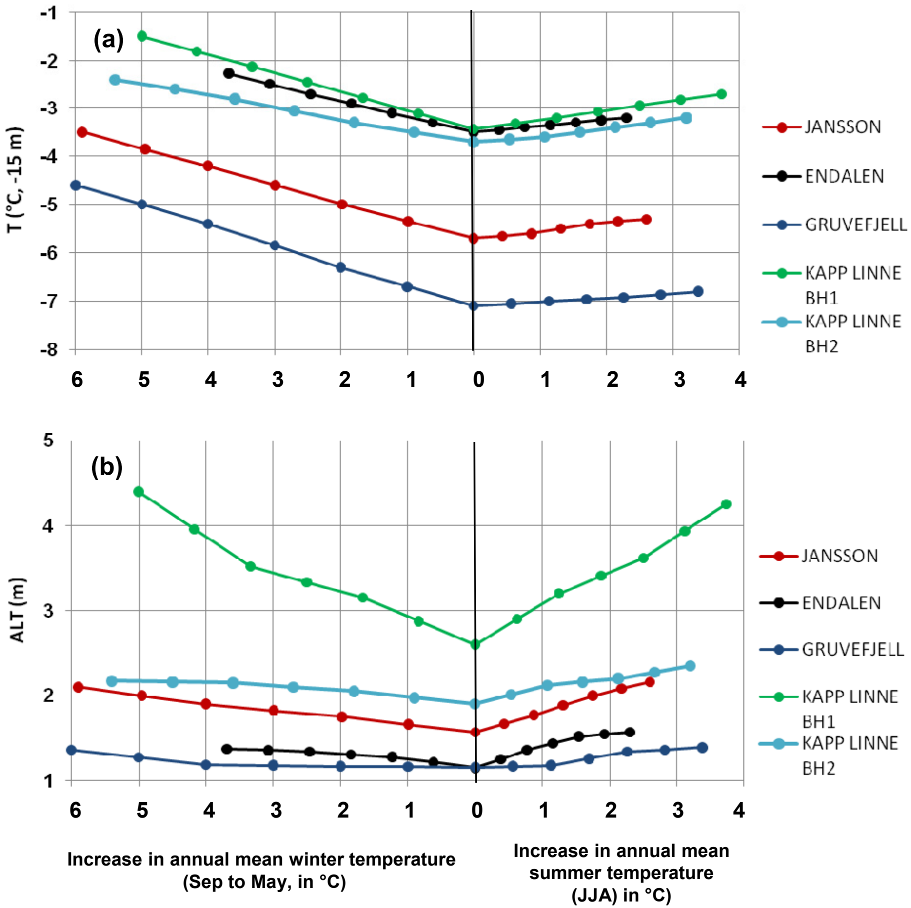

Fig. 7. Impact of GST changes during summer (JJA) and fall/winter/spring (September to May) on ground temperature in 15 m depth **(a)** and on ALT **(b)** for the different study sites. The model was then run over a period of 10 years and the presented results are the differences to the undisturbed values.

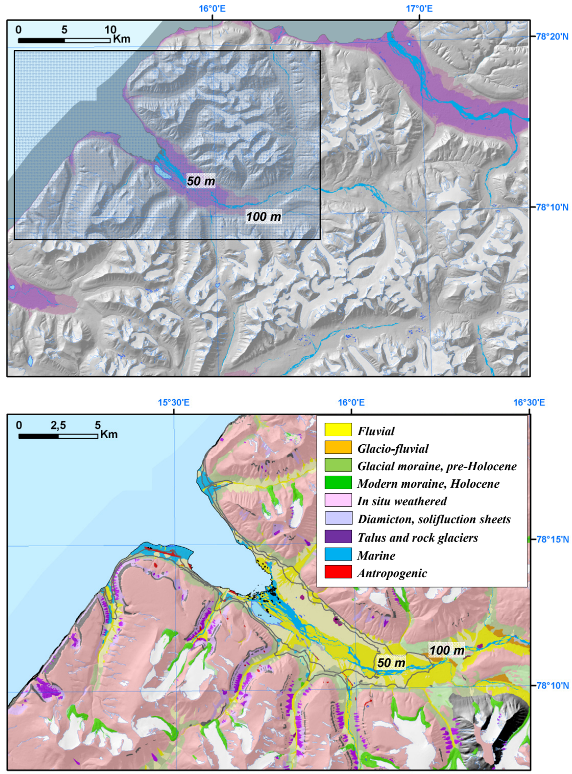

Fig. 8. **(a)** Hillshaded map of the Adventdalen area and surroundings. The two violet colours denotes the 50 m and 100 m contour line, respectively. Large areas within the valley bottoms draining to Isfjorden are lying within this zone. **(b)** Geomorphological map over the area around Longyearbyen (based on Tolgensbakk et al., 2000). The gray lines denote the contours from above. The area below 50 m is mainly consisting of marine sediments, beach deposits, fluvial infilling, slope sediment such as gelifluction colluviums, alluvial fans and some singular bedrock outcrops, mainly in steep rock walls or coastal cliffs.

TCD
4, 1877–1908, 2010

Modelling past and future permafrost conditions in Svalbard

B. Etzelmüller et al.